Experimental Investigation on Onset Criteria of Liquid/Gas Entrainment in the Header-Feeder System of CANDU

Jae Young Lee*, Gi-Suk Hwang
Department of Mechanical Engineering, Handong Global University, Pohang 791-708, Korea
Manwoong Kim
Korea Institute of Nuclear Safety, 19, Daejeon 305-338, Korea

An experimental study has been performed to investigate the off-take phenomena at the header-feeder systems (horizontal header pipe with multiple feeder branch pipes) in a CANDU (CANadian Deuterium Uranium) reactor with the branch orientation varies $\pm 36°$ or $\pm 72°$. In order to evaluate the applicability of the conventional correlations used in the safety analysis code, RELAP5-Mod3, the test facility is designed with the 1/2 scale of the CANDU 6. It was found that the data set for the top, bottom and side branches are in a good agreement with the correlations used. However, for the specific angled branches, $\pm 36°$ and $\pm 72°$, the onsets of off-take data and quality data showed large deviation with the conventional model inside RELAP5-MOD3. Furthermore, based on the uncertainty analysis, the conventional 2.5 power law needs to be modified. The present experimental data set can be useful for the construction of the general correlation considering the arbitrary branch orientation.

Key Words : Off-Take, Liquid Entrainment, Gas Pull Through, Froude Number, CANDU

Nomenclature

D,d : Diameter of header and diameter of branch pipe
Fr : Froude number
g : Gravitational acceleration
h : Water level
j : Volumetric velocity
q : The gas volumetric flow
Q : The volume flow rate
r : The rise of water level at the wall
V : Velocity
x : The quality

Greek

α : The void fraction
δ : The wave height
λ : Wave length
ρ : The density
$\Delta\rho$: $\rho_f - \rho_g$

Superscript

$*$: Dimensionless

Subscript

b : Onset condition
g : Gas
3g : The gas phase at the branch
R : Ratio of prototype to the reference

* Corresponding Author,
E-mail : jylee7@handong.edu
TEL : +82-54-260-1392; **FAX** : +82-54-260-1392
Department of Mechanical Engineering, Handong Global University, Pohang 791-708, Korea. (Manuscript **Received** August 11, 2005; **Revised** April 18, 2006)

1. Introduction

A lot of industrial applications involve two-phase flow discharging from a stratified region through single or multiple branches. For instance, these applications include the flow through small break in horizontal cooling channels of a CANDU reactor during postulated loss-of-coolant accidents (LOCA), the flow distribution at the

header-feeder systems during accidents and two-phase distribution headers, where a certain incoming stream fed into a large header is divided among a number of discharging stream. Therefore, knowledge of the flow phenomena including the mass flow rate and quality of all discharging streams is obviously essential for the design and safety analysis of such system.

For the case of single discharge from a large flow channel under stratified flow conditions, Zuber (1980) pointed out that the phenomena of gas and liquid entrainment will influence the flow through the branch. He proposed simplified correlations for the onsets of these phenomena in terms of relevant system parameters and branch orientation (top, bottom or side) depending on the location of the gas-liquid interface relative to the branch. If the interface is located above the branch, gas can be entrained by vortex or vortex-free motion into the predominantly liquid flow through the branch. On the other hand, if the interface is located below the branch, liquid may be entrained into the predominantly gas flow. Later, detailed experiments were conducted on the onsets of gas and liquid entrainment, two-phase mass flux and quality during discharge from a large stratified region through a single branch with different orientations by Smoglie (1984) and Reimann et al. (1984), Schrock et al. (1986), Yonomoto and Tasaka (1988).

The off-take problem has been formulated in the form of correlation into the safety analysis code through the intensive experimental and theoretical works during the last decades. For instant, RELAP5/MOD3, a best estimate safety analysis code, involved the liquid entrainment and vapor pull-through models of a vertical and horizontal pipe for predicting branch quality of T-junction. In the CANDU reactor, there are two difficulties associated with the arbitrary orientation of branch pipes and the number of tubes. Since the current off-take model in the RELAP5/MOD3 is made for the single branch tube with the specific orientation such as the top, bottom, and side orientations, simple interpolation of the existing correlations cannot be the solution for the header and feeder pipes in CANDU reactors. The designs of the CANDU reactors are different from those of the light water cooled reactors (LWR). For example, a lot of the pressure tubes penetrate the CANDU reactor and include the fuel bundles. A total of 380 fuel bundles divided into the four groups with 95 fuel bundles respectively and are connected with the feeder pipes in order to transport the coolant for heat exchange. Especially, there are five-angled types at T-junctions between header and feeder pipes ; 0°, 36°, 72°, 108°, 144° from the horizontal line. Unfortunately, the current horizontal stratification entrainment model in RELAP5/MOD3.3 cannot predict the exact mass qualities at specific angle branches because it can be applied only at the bottom, top and side branches. The geometrical characteristics between the header and feeder pipes of the CANDU reactor require different approaches to safety analysis from the existing simulation codes developed for LWRs.

Unfortunately, the researches for the off-take phenomena in the branch pipes with arbitrary angle were, however, hardly to find and there is no reliable correlation for this purpose. During the last decades, several models and correlations were developed by experimental studies. KfK (Smoglie, 1984) reported the results of experiments designed to determine the mass flow rate and quality through a small break at the bottom, top and side of a main pipe with stratified gas-liquid flow. The break diameters are 6, 8, 12, 20 mm respectively and the main pipe diameter is 206 mm. These experiments were performed with air-water flows at ambient temperature and a maximal pressure of 0.5 MPa. UCB (Schrock et al., 1986) also presented the results of an experimental investigation of air-water and steam-water discharges from a stratified upstream region through small diameter breaks oriented at the bottom, top and side of the horizontal pipe. The main pipe was 102 mm in diameter and the break tubes were 4, 6, and 10 mm in diameter respectively and 123 mm in length. Both air-water and steam-water were used at pressures up to 1.07 MPa. These two experimental results are implemented into the horizontal stratification entrainment model (HSEM) in RELAP5/MOD3.3, which

accounts for the phase separation phenomena and computes the onset and the quality of liquid and gas entrainment at branches attached to a horizontal pipe.

In the present study, to investigate the off-take phenomena for a single branch with the arbitrary angle, off-take experiments are carried out using the experimental facility of the horizontal pipe with 7 angled branch pipes. The header and feeder pipes in CANDU 6 are designed as the 1/2 scaled-down off-take test facility. The onset of liquid/gas entrainments and qualities at the branch entrance for stratified flow in the horizontal pipe are compared with the previous experimental results, KfK and UCB. In addition, the off-take phenomena at branch pipes with four specific angles as well as three branches (top, side and bottom) are also described.

2. Previous Studies

In the present section, a brief introduction of the previous models for the off take phenomena is made. It has been generally accepted that the water level at the onset condition of the entrainment,, is the key parameter in termination of the exit quality and mass flow rate through the branch pipe and it is correlated with the Froude number which is the function of the velocity of the continuous phase in the branch pipe. The general form accepted to describe the onset condition of entrainment was given by Rouse (1956) developed a correlation from the experiments of the non-circulatory waterspout

$$Fr_g\left(\frac{\rho_g}{\Delta\rho}\right)^{0.5}=C_1\left(\frac{h_b}{d}\right)^{C_2} \tag{1}$$

where Fr is the Froude number, $Fr_g=V_{3g}/\sqrt{gd}$, V_{3g} is the velocity of the continuous phase in the branch pipe, D is the diameter of header, and d is the diameter of the branch pipe. The constants C_1 and C_2 were determined by fitting the experimental data.

The first theoretical work to model the phenomena was made by Craya (1949) for the onset of the liquid entrainment at the side branch at the water reservoir. Later it was verified by the experimental works of Gariel (1949) and Crowely and Rothe (1981). As depicted in Fig. 1, the side branch flow bring the water to rise the level at the wall, r. Ignoring the surface tension and viscous force at the water surface, the application of the Bernoulli relation with the assumption that $r=4h/5$, Craya developed the onset condition as

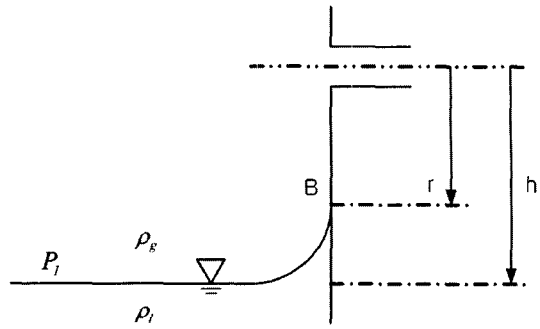

Fig. 1 The schematic drawing the liquid entrainment t the side branch

$$h_b=K\left[\frac{\rho_g q^2}{g\Delta\rho}\right]^{0.2} \tag{2}$$

where, q is the gas volumetric flow rate to the branch and K is determined as 0.68.

The model of Craya has the meaning as the first investigation but the diameter of branch pipe was neglected in the correlation. The first model accounting the diameter effect was made by Rouse (1956) who developed a correlation from the experiments of the non-circulatory waterspout. His correlation of the dimensionless water level number (h_b/d) to the Froude number, $Fr_g=V_{3g}/\sqrt{gd}$, as Eq. (1) is the general form of onset conditions developed. Zuber (1980) accepted the correlation reasonably for the scaling of the break-out flow through the broken pipe. Eq. (1) has been used as the standard form in the modeling of the onset condition at the top, bottom, and side branch flow. Crowley and Rothe (1981) determined the constants C_1 and C_2 experimentally as 3.25 and 2, respectively. In line with the experimental works of KfK for the top, bottom, and side branch form the horizontal pipe with the stratified flow, Smoglie (1984) developed a correlation based on the potential flow theory as illustrated in Fig. 2 in which the branch pipe was treated as

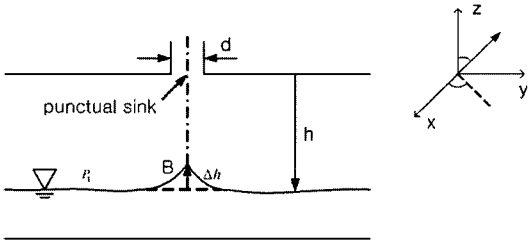

Fig. 2 The schematic drawing of the liquid entrainment at the top branch

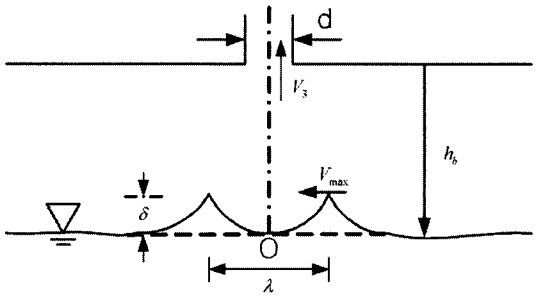

Fig. 3 The schematic drawing the liquid entrainment at the top branch with the two waves at the onset condition

the punctual sink point. The theoretically derived constants were, C_1=3.25, C_2=2.5, but Smoglie determined them from the experimental data as C_1=0.353, C_2=2.5. It was interesting that the 2.5 power law was theoretically derived, C_1=25 and C_1 coefficient of experimental data was 1/10 of the theoretical value. As Reimann and Khan (1984) noted through their experimental work, the model has limitation of not counting the diameter ratio of d/D. Furthermore, Schrock et al.(1986) performed experimental works and determined constants as C_1=0.395 and C_2=2.5, which is very similar to the results of KfK. In this point of view, the 2.5 power law has been widely accepted in the correlation of the onset condition.

However, another noteworthy approach was made by Maciaszek et al.(1989) of CENG, in which they took account of the water waves at the onset condition which has the distance of λ as depicted in Fig. 3.

They followed the original proposal of Bharathan et al.(1982) based on the continuity and potential flow theory to determine the wave height as $\delta=1/3h_b$, In their determination of the wave height, the instability theory was adopted and counting λ as the diameter of the branch pipe d and determined the constants as C_1=1.54, C_2=1.5. Therefore, the instability model of Maciaszek et al. departs from the general 2.5 power law. In the present study, the experimental data set measured will be used to check the proposed correlations and to see how much depart the data of the specific angled cases from them.

3. Experimental Facility

The scaling analysis is performed to design the off-take test facility on the prototype of CANDU6. The major scaling parameters are the diameter (D) and length (L) of the header pipe and the diameter of the feeder pipes (d). The phenomena related to the off-take are considered in the scaling analysis: flow regime in the horizontal pipe and the onset of off-take at the branch pipes.

At first, the diameter of the horizontal pipe (D) is scaled down as 1/2, which results in 0.184 m as the value of D. For the countercurrent flow limitation, it has been generally considered that L/D plays an important role, but in the study it is just recommended as an important parameter for the scaling design. This is partially due to the fact that the actual header pipe has various lengths according to the locations of each feeder pipe. Therefore the length of the horizontal pipe is designed to be suitable of the experimental conditions. The flow rates inducing an off-take are related to the Froude number in case of the horizontal stratified flow. Basically, the void fraction is preserved in horizontal stratified flow: geometrical similitude. Since the multiplication of the Froude number to the void fraction is the volumetric flow rate of Wallis for the countercurrent flow limitation. In the present scaling we used the scaling index $[Fr\cdot\alpha]_R$=1. Also, the branch quality need to be preserved, ($[x]_R$=1). These two criteria gave us volumetric flow and the branch diameter based on the scale of the header diameter: $[Q_k]_R=[D^{5/2}]_R$ and $[d]_R=[D^{5/4}]_R$. The branch pipes are designed into three diameters scaled down from the feeder pipes on

Table 1 Summary of the test facility compared with a CANDU-6 reactor

	CANDU6	Test Facility	Scaled-down Ratio
Header diameter [m]	0.3683	0.184	0.5
Header length [m]	6.00	0.8	0.133
Feeder diameter-1 [cm]	3.81	1.60	0.420
Feeder diameter-2 [cm]	4.93	2.07	0.420
Feeder diameter-3 [cm]	5.90	2.48	0.420
Gas/liquid flow rate			0.177

the basis of the above scaling result. Table 1 summarizes the scale of the test facility compared with the prototype (CANDU6). Figure 4 shows the overall schematic diagram of the test facility, which consists of air-water tank, horizontal pipe, branch pipes having three different diameters, air-water separator and collecting tank of entrained water. Additionally, the air compressor, water pump, their control panel sets and various measuring instruments are installed to the test facility. The horizontal main pipe and the branch pipe are scaled down to represent the header pipe and the feeder pipes of the CANDU 6 reactor, respectively as listed in Table 1. The major scaling parameter used was the Froude number. All the test facility is made of stainless steel as a design pressure of 10 bar. Visual windows are installed for observation in the T-junction in the horizontal main pipe and air-water separator. At the T-junction, the circular branches with diameters of 16, 20.7, 24.8 mm can be installed and removed for different branch diameters and angles. The branch angles are 0°, 36°, 72°, 90° from the horizontal line and illustrated in Fig. 5. The diameter and length of the horizontal pipe are 184 mm and 775-1,035 mm, respectively. The honey-comb at the inlet of the horizontal main pipe is installed for flow stabilization. Compressed gas and water flows are supplied by the air compressor and water pump, respectively. In the case of a liquid entrainment, the two-phase branch flow is separated into entrained water and gas flow in the air-water separator. Thereafter, the entrained air/water is collected and measured by different methods according to the amount of those. Water levels in the horizontal pipe are measured at both

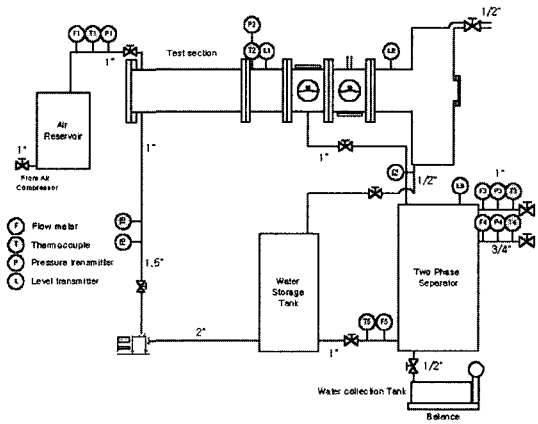

Fig. 4 Schematic diagram of the test facility

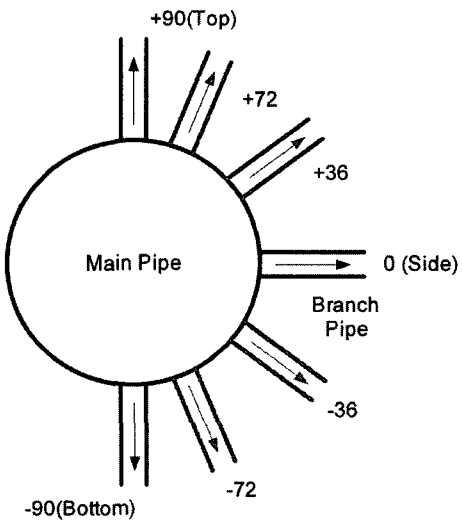

Fig. 5 Side-view of T-junctions

front and real positions of the T-junction. For circulating quality, water level in the air-water separator was measured. Orifice-meters and vortex-meter are used for measuring air flow rates

Table 2 Summary of experimental studies

Investigator	D (m)	D/d	Working Fluid	Branch Orient
Reimann and Khan (1986) (KfK)	0.206	34.3, 25.7, 17.1, 10.3	Air-Water	Top, Side, Bottom
Schrock et al.(1986) (UC-Berkeley)	0.102	27.2, 25.8, 16.1, 10	Air/Steam-Water	Top, Side, Bottom
Moon and NO (2000) (KAIST)	0.295	5.9, 4.2	Air-Water	Top
Hwang and Lee (2002) (HGU-KINS)	0.184	11.5, 7.4	Air-Water	Top, Side, Bottom

and magnetic flow meters are installed in order to measure water flow rates.

The experiment is performed at room temperatures and maximal pressure of 8 bar. The maximum air flow rate and water flow rate used in the tests is up to 70×10^{-3} kg/s and 3.5 kg/s, respectively. Water levels in the horizontal pipe can be controlled by inlet/outlet valves of flow pipes, controlling water pump power and dam in outlet the horizontal pipe. To obtain the data of the onset of liquid/gas entrainment, the input and branch mass flow rate of air/water are fixed and the interface level increases/decrease very slowly (1 mm/min). Therefore, the experiments can be assumed to be at steady state. All injected air/water are discharged through the branch pipe because of no exit flow in the horizontal pipe. In Table 2, recent experimental studies are summarized.

4. Results and Discussions

A series of experiments was performed to confirm that the present facility produces similar data as the previous experimental data by KfK and UCB for the top, bottom, and side branches. Also, the off-taking onset data for the branches with ±36, $\pm72°$ were measured. The experiments of onset conditions for branch flow were measured with three different diameter and seven different orientations for the branch pipes respectively as shown Table 3. The operating pressure was maintained up to around 8 bar and the air and water flow rates are up to 0.07 kg/s and 3.5 kg/s, respectively.

4.1 Onset of liquid entrainment at top branches

As for the top branch, it is observed that the water surface changed as the water level increases. As shown in Fig. 6, the dimple size grows up as the water level increases. Also, the instability on the surface of the dimple suddenly produces many droplets which will entrained into the branch pipe (Fig. 6.(c)). The onset condition was set to this case.

The present experimental data of OLE were plotted in Fig. 7. The solid circles denote the OLE for 16 mm diameter branch pipe and the solid rectangle represented the OLE of 24.8 mm. The experimental data are partially scattered due to the instability at the interface of the water as well as the vortex near the wave crest. The present experimental data are close to those of KfK presented with the white circle for 6 mm diameter branch, white triangle for 12 mm diameter branch, and white rectangle for 20 mm diameter branch. Also, experimental data of the present and KfK data are well converged to the correlation of RELAP5/MOD3 which represented 2.5 power law. Comparing with UCB experimental data, the present experimental data are a little deviated to the left side from the UCB data and the conventional correlation while the data of UCB for the lower Froude number approached to those of KfK and the present experiment. It can be said that the experimental data support the 2.5 power law. However, as listed in Table 4, the best fitting of the experimental data produced scattered values of C_2 are scattered in the range of 1.63-2.8 in accordance with D/d. Comparing

Table 3 Test matrices for the onset of entrainment experiments

Entrainment type	θ (°)	d (mm)	P (MPa)	$\dot{m}_g$ or $\dot{m}_l$ (kg/s)	h_b/d	# of data
	+90 (top)	16, 24.8	0.226-0.808	6.2-70.9	0.92-3.4	17
	+72	16-24.8	0.255-0.810	4-79	1.31-3.04	34
G.E.	+36	16-24.8	0.188-0.674	21.7-75.9	0.94-2.4	40
	0 (side)	16, 24.8	0.177-0.541	16.3-67.7	0.7-1.81	18
	−36	16-24.8	0.158-0.609	15.1-84.2	0.75-1.58	50
	+36	16-24.8	0.133-0.547	0.32-3.04	0.81-1.84	43
	0 (side)	16, 24.8	0.137-0.758	0.46-3.66	0.78-3.18	26
L.E.	−36	16-24.8	0.334-0.810	0.57-3.09	2.64-7.39	43
	−72	16, 20.7	0.304-0.810	0.63-2.6	5.5-10.17	34
	−90 (bottom)	16, 24.8	0.397-0.804	1.26-3.3	5-10.85	29

Table 4 Summary of uncertainty analysis results on the empirical constant, C_2 for OLE at 90°

Investigator	d (m)	D/d	C1	C2	Deviation Rate (%)
KfK	0.006	34.3	1.132	1.63	−34.8
	0.012	17.1	0.352	2.44	−2.4
	0.020	10.3	0.295	2.8	12.0
UCB	0.00376	27.2	0.27	2.67	6.8
	0.00396	25.8	1.794	1.67	-33.2
	0.00632	16.1	0.474	2.45	-2.0
KAIST	0.05	5.9	0.277	2.5	0.0
	0.07	4.2	0.497	2.034	-18.6
HGU-KINS	0.016	11.5	0.389	2.316	-7.4
	0.0248	7.4	0.77	2.106	-15.8

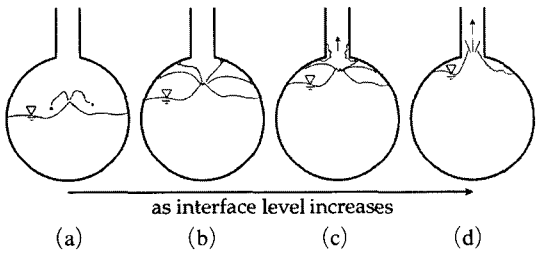

Fig. 6 Development of liquid entrainment at the top branch

with 2.5 power law, it shows that the uncertainty are increased up to −34.8% and the average uncertainty is about 16%.

4.2 Onset of gas entrainment at the bottom branches

The onsets of gas entrainment (OGE) and gas

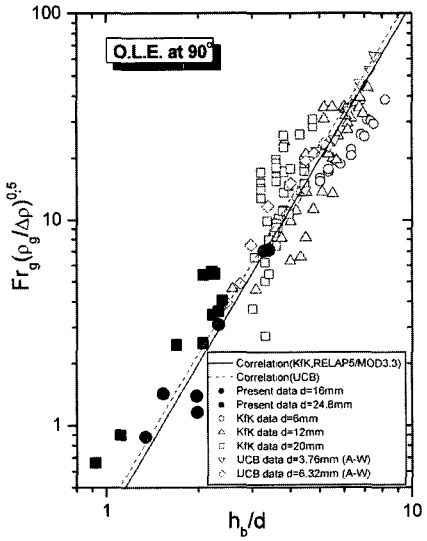

Fig. 7 Comparison of OLE data at the top branch with the experimental data

pull through are measured at the bottom branch and side branch in which water level is higher than the center line of the side branch. For the bottom branch, when the liquid are ejected out through the bottom branch, a dimple at the interface of the water was observed. When the water level reaches to the certain level, the dimple-type air flows to the bottom branch. In this study, three typical phenomena as shown Fig. 8 are considered to decide the definition of OGE (onset of gas entrainment). As the water level decreases, the dimple at first produces very tiny bubble which pulled through the branch pipe and for the lower water level a gas hose produced and finally it grow up and gas swept out as the vortex free condition. In this case the definition of the onset condition is very subjective to the researcher. Also as shown in Fig. 9, the experimental data between KfK and UCB show a large deviation. Therefore, in the present study, we used the sudden increase of quality at the branch pipe which is measured by the impedance meter.

In Fig. 9, the present experimental data are close to the data and correlation of KfK while the correlation of RELAP5/MOD3.3 is located in between the UCB and KfK and the correlation of UCB has different slope. The reason of this deviation came form the definition of OGE since UCB adopted the definition of OGE as the first bubble pull through as shown Fig. 8(a). In the meanwhile, the new definition based on the quality rise at the branch pipe is proposed in such a way to consider the safety perspective. If the unstable situation of the first bubble pull through is adopted as the definition of the OGE, the ambiguous observation will produce some confusion which is already represented in the correlation. RELAP5/MOD3 accepted the middle of the UCB and KfK but still kept the 2.5 power law. In this point of view, it implies that RELAP5/MOD3.3 has

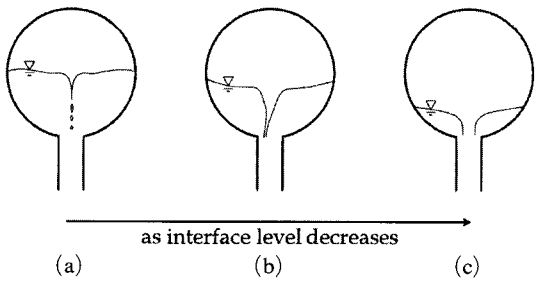

Fig. 8 Development of gas entrainment at the bottom branch

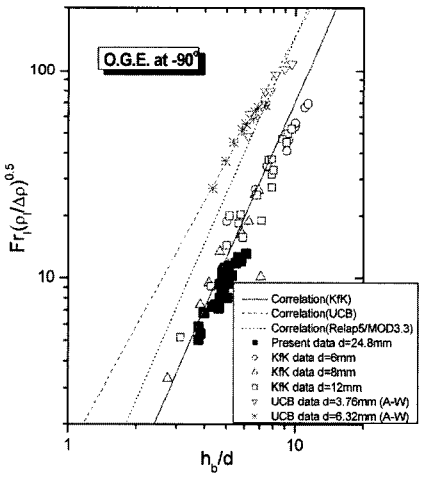

Fig. 9 Comparison of OGE data at the bottom branch with the experimental data

Table 5 Summary of uncertainty analysis results on the empirical constant, C_2 for OGE at −90°

Investigator	d (m)	D/d	C1	C2	Deviation Rate (%)
KfK	0.006	34.3	1.33	1.60	−36.00
	0.012	17.1	0.47	2.07	−17.40
	0.020	10.3	0.64	1.80	−28.00
UCB	0.00376	27.2	2.49	1.70	−32.00
	0.00632	16.1	2.13	1.78	−28.80
	0.00376	27.2	0.65	2.03	−18.64
	0.00632	16.1	2.38	1.32	−47.20
HGU-KINS	0.0248	7.4	0.46	1.89	−24.40

the reasonable correlation for the OGE. As listed in Table 5. the best fit gave us the values of C_2 are scattered in the range of 1.32-2.07 in accordance with D/d. Comparing with 2.5 power law, it shows that the uncertainty are increased up to −47.2% and the average uncertainty is about 30%.

4.3 *Onset of liquid/gas entrainment at side branches*

4.3.1 Onset of liquid entrainment

As for the side branches, as a gas flow increases, the liquid entrainment at side branch occurs as shown Fig. 10(a). The Bernoulli effect is evidenced by the deflection of the interface in the vicinity of the branch wall first but disappears again like Fig. 10(b). With further increase of the liquid level, a thin ascendant film of water, not influenced by vortex, determines the onset of liquid entrainment. The liquid vortex on the interface level can be hardly observed because of the inner wall friction in the horizontal pipe as shown Fig. 10(c). Finally, a lot of the entrained liquid is discharged intermittently or continuously. In this study, the OLE is defined in the case of Fig. 10(b).

In Fig. 11 is shown the OLE at the side branch of the present experiment is on the line of the existing correlations: RELAP5/MOD3.3. The present data are well agreed with the previous experimental data of KFK and UCB. While UCB data has a little scattering, the correlation proposed by UCB agrees with that of KfK. Therefore, for the OLE at the side branch, the present experimental data support the existing data and correlation firmly so that no more effort to develop the correlation is needed in this case. But the best fit data in table 6 gave the values of C_2 are scattered in the range of 2.03-3.05 in accordance with D/d. Comparing with 2.5 power law, it shows that the uncertainty are increased up to ±22% and the average uncertainty is about 16%.

4.3.2 Onset of gas entrainment

In Fig. 12, three phenomena for the side branch were observed. Figure 12(a) illustrated that as a liquid flow increases the continuous liquid phase generates a very small vorticity. However, this small vorticity is difficult to be observed and then disappears rapidly. As the liquid increases, thin gas hose forms in the vicinity of the branch and small bubbles are discharged through the branch. The wall friction prevents the vorticity from developing and after short intermittences the gas is in direct contact with the wall as shown Fig. 12 (b). Figure 12(c) shows that as increase of liquid

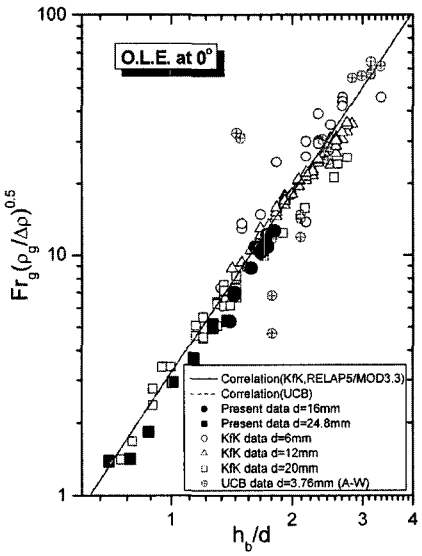

Fig. 11 Comparison of OLE data at the side branch with the experimental data

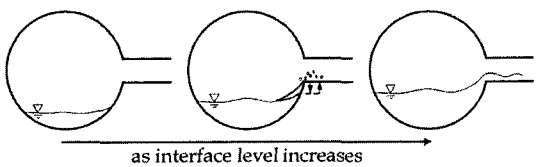

Fig. 10 Development of liquid entrainment at the side branch

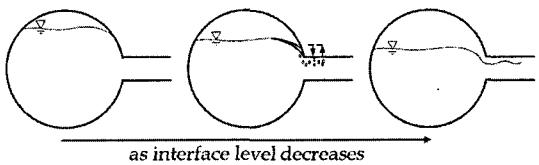

Fig. 12 Development of gas entrainment at the side branch

flow the more gas is swept out instead of vortex flow.

HSEM in RELAP5/MOD3.3 predicts reasonably the data although they are scattered around the correlation shown as Fig. 13. The data of UCB shows large scattering and the correlation

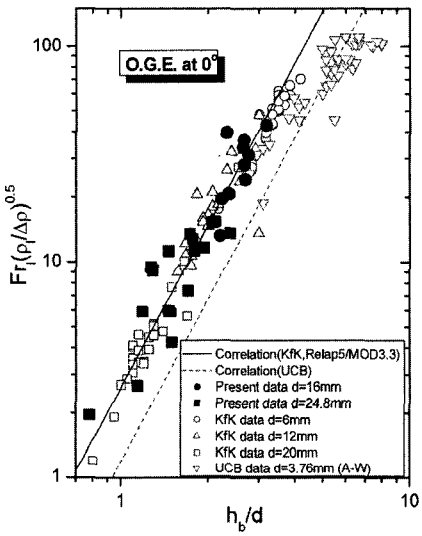

Fig. 13 Comparison of OGE data at the side branch with the experimental data

may not well fitted by the data. Some data for Froud number, Fr, around 50 approached to those of the KfK data, which shows very consistent tendency of the 2.5 power law and correlation. For the OGE of the side branch, since the present experimental data are good agreement with those of the KfK data and correlation, the present study reconfirmed the validity of the correlation of RELAP5/MOD3. In Table 7, the values of C_2 are scattered in the range of 1.19-2.38 in accordance with D/d. Comparing with 2.5 power law, it shows that the uncertainty are increased up to -52.5% and the average uncertainty is about 25%.

4.4 Onset of liquid/gas entrainment at ±36°, ±72°

4.4.1 Onset of liquid entrainment

In addition to the above experiments, to grasp the angle effect, the off-take experiments for specific angled (±36°, ±72°) branches were carried for CANDU 6. As for +72° branch, the onset of liquid entrainment is quite similar to the case of +90° in which the vortex formed and suddenly

Table 6 Summary of uncertainty analysis results on the empirical constant, C_2 for OLE at 0°

Investigator	d (m)	D/d	C1	C2	Deviation Rate (%)
KfK	0.006	34.3	4.83	2.12	−15.20
	0.012	17.1	4.46	2.03	−18.80
	0.020	10.3	3.33	2.11	−15.60
UCB	0.00376	27.2	4.43	2.09	−16.40
HGU−KINS	0.016	11.5	2.17	3.05	22.00
	0.0248	7.4	2.75	2.28	−8.80

Table 7 Summary of uncertainty analysis results on the empirical constant, C_2 for OGE at 0°

Investigator	d (m)	D/d	C1	C2	Deviation Rate (%)
KfK	0.006	34.3	3.27	2.20	−12.00
	0.012	17.1	4.53	1.82	−27.20
	0.020	10.3	2.56	2.38	−4.80
UCB	0.00376	27.2	5.15	1.49	−40.40
	0.00376	27.2	4.84	1.19	−52.44
HGU−KINS	0.016	11.5	3.30	2.25	−10.00
	0.0248	7.4	3.65	1.84	−26.40

broken up into liquid droplets. The first touch of the liquid droplet into the branch was defined the onset condition. However, as for the ±36° the onset condition is quite similar to the side branch case. We cannot find isolated solitary wave, however, the end of the water wave touched the branch and flowed into the branch. The experimental data were tested to know how much they are apart form the existing data and to know is it possible to interpolate the existing correlations using additional parameter such as the angle of branch orientation θ. It may need more experimental works to produce the unified correlation taking account of the angle effect. At this moment, the presentation of the data and simple discussions are made in the present section.

For the branches with ±36°, +72°, the liquid entrainment phenomena were observed. The data for all three diameters of branches were obtained. It is observed that the off-take phenomena from the interface for the branches with +72° are similar to those at top branch and those at side (0°) and −36° branches are almost the same. But it is difficult to observe the vorticity on the interface at the branches with +36° because the inner wall in the horizontal pipe hinders its formation. A small deviation from HSEM in RELAP5/MOD3.3 is found as shown in Fig. 14. The data are fitted closely to the correlation at the top branch for the branch with +72°. However, the data for the branches with ±36° are close to the correlation at the side branch because the inner wall in the horizontal pipe influences the onset of entrainment like the side branch. Especially, the data at branches with +72°, +36° are the correlation at the between top and side branch because friction in the inner wall of the horizontal pipe and the entrainment from the interface determine simultaneously the onset of entrainment.

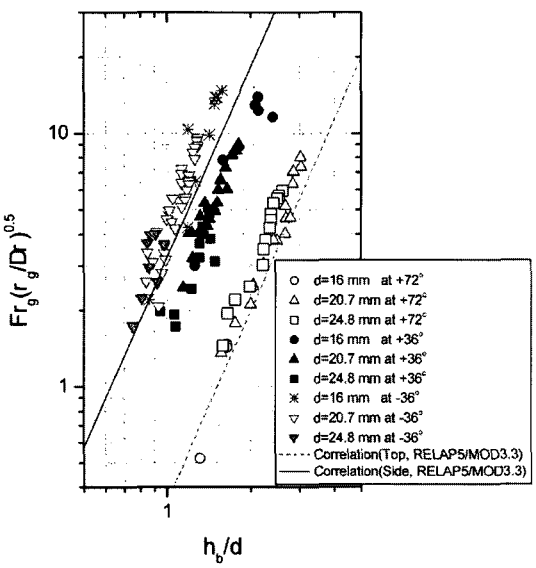

Fig. 14 Comparison of the O.L.E. data at +72°, ±36° branches with the experimental data

4.4.2 Onset of gas entrainment

As for −72° branch, the phenomena of the gas entrainment is quite similar to the case of −90° in which the vortex of the gas stream made a swirl flow and finally touched down the branch. For −36°, still we are able to observe similar vortex but smaller than −90° and −72° branches. Onset of gas entrainment in this case occurs more earlier than those cases. However, as for +36°, the onset of the gas entrainment occurred very near the side branch. The shape of the water surface is very similar to that of the side branch. The definition of the first gas hose as the onset of gas entrainment cannot be applied to the branch with ±36°, −72° because it is difficult to observe the first gas hose phenomena in specific angled branches unlike the bottom branch so that the first bubble gas entrainment was used as the definition of OGE. As depicted in Fig. 18, the present data with the definition of the first bubble entrainment were plotted. The data of bottom branch with the definition of the first gas hose also plotted for the comparison. Phenomena at branches with +36° are similar to those at side branch ; those at both bottom and −72° branches are almost the same. There are no differences between bottom branch and −72° branch are shown in Fig. 15.

However, a deviation between HSEM of the side branch in RELAP5/MOD3.3 and the data at the branch with +36° is seen clearly. The data at the branch with −36° are on the line of the correlation developed by the KfK, however, they are away from the data at the branches with −72°, −90°. Like the onset of liquid entrainment, the

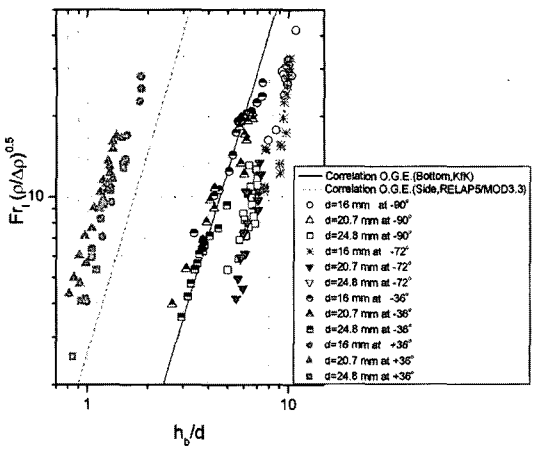

Fig. 15 Comparison of the OGE. data at $-72°$, $\pm 36°$ branches with the experimental data

inner wall in the horizontal pipe influences the data at the branch with $-36°$. From this, it was found that for the gas pull through there are two attracting lines of the side branch and bottom braches where the data set approach.

4.5 Uncertainty analysis

A study used here for estimating uncertainty in experimental results was presented by Coleman and Steele. Consider a general case in which an experimental result, r, is a function of N variables X_i

$$r=r(X_1, X_2, \cdots, X_N) \tag{3}$$

Equation (A-1) is the data reduction equation used for determining r from the measured values of the variables X_i. Then the uncertainty in the result is given by

$$U_r=\left[\left(\frac{\partial r}{\partial X_1}U_{X_1}\right)^2+\left(\frac{\partial r}{\partial X_2}U_{X_2}\right)^2+\cdots+\left(-U_{X_N}\right)^2\right]^{1/2} \tag{4}$$

where U_{X_i} are the uncertainties in the measured variables X_i.

Here, the uncertainties in gravitational constant and geometrical factors such as diameters of horizontal pipe and branch pipes and angles of branch pipes are ignored. And present experiment was performed at ambient temperature so the uncertainty in the liquid density is ignored additionally. However, Air density has the 0.002% due to 0.2% uncertianties of temperature measurement. Air mass flow rate was measured by the vortex flow meter with 1% error. Liquid mass flow rate was measured by the magnetic flow meter with the uncertainties of 0.5%. Therefore the major factor to determine the on set condition is the inception height:

$$h_{b,k}=C\left[\frac{W_k}{\sqrt{g\rho_k\Delta\rho}}\right]^{0.4} \tag{5}$$

Then the uncertainty in $h^*_{b,k}$ is as follows:

$$\left(\frac{\Delta h_{b,k}}{h_{b,k}}\right)=\left[(0.4)^2\left(\frac{\Delta W_k}{W_k}\right)^2+(-0.2)^2\left(\frac{\Delta\rho_k}{\rho_k}\right)^2+(-0.2)^2\left(\frac{\Delta(\Delta\rho)}{\Delta\rho}\right)^2\right] \tag{6}$$

The uncertainties in $h^*_{b,k}$ for gas and liquid entrainments are 0.72% and 0.41% respectively.

5. Conclusions

In the present study, the off-take phenomenon at $\pm 36°$, $\pm 72°$ angled branches including top, side and bottom branches in the horizontal pipe are experimentally investigated. The experimental facility with 1/2 scale of the header pipe and feeder pipes in the CANDU reactor was designed and constructed to produce the onset conditions. Besides, to analyze the uncertainty of the empirical constant, C_2, comparing with 2.5 power law, four experimental results are formulated in accordance with D/d and derived the empirical constants C_1 and C_2 respectively. As the results of this study, it is concluded as follows:

(1) As for the typical branches such as top, bottom and side branch, the experimental data were a good agreement with those of the KfK data and the existing correlation in RELAP5/MOD3.3.

(2) As for the OLE at the arbitrary angled branches such as $\pm 36°$, $\pm 72°$, the branch angle effect was clear, however, it needs some improvement the OGE for $\pm 36°$ are close to OGE of the side branch but data of $+72°$ branch are close to the top branch.

(3) As for the OGE, the OGE at the $+72°$ branch are close to the bottom branch. But for those of $+36°$ and $-36°$ branch are lined to the left and right side of the side branch data.

(4) According to the uncertainty analysis for the empirical constants, C_2, with 2.5 power law, it could be concluded that in the correlations for the liquid and gas entrainments, the 2.5 power law needs modification adequate to the empirical constants, C_2.

In the present study, it could be improved the new onset data of the gas/liquid entrainments at the $\pm 36°$, $\pm 72°$ angled branches. However, it was also concluded that more experimental works for the branches with arbitrary angle and the effort to develop general correlation respecting the branch angle are imperative for safety analyses of CANDU reactors.

Acknowledgments

This research was performed under the program of Basic Atomic Energy Research Institute (BAERI) supported by the Ministry of Science & Technology (MOST) of Korea.

References

Bharathan, D., Wallis, G. B. and Richter, H. J., 1982, "Lower Plenum Voiding," *J. of Heat Transfer*, Vol. 104, pp. 479~86.

Craya, A., 1949, "Theoretical Research in the Flow of Non-homogeneous Fluids," *La Houille Blanche*, pp. 44~55.

Crowley, C. J. and Rothe, P. H., 1981, "Flow Visualization and Break Mass Flow Measurements in Small Break Separate Effects Experiments," *Proc. of ANS Specialist Meeting in SBLOCA in LWRs*, Monterey.

Gariel, P., 1949, "Theoretical Research in the Flow of Non-homogeneous Fluids," *La Houille Blanche*, pp. 56~64.

Maciaszek, T. and Micaelli, J. C., 1989, "The CATHARE Phase Separation Model in Tee Junctions," SETH/LEML-EM/89-159.

Reimann, J. and Khan, M., 1984, "Flow through a Small Break at the Bottom of a Large Pipe with Stratified Flow," *Nuclear Science and Engineering*, Vol. 88, pp. 297~310.

Rouse, H., 1956, "Seven Exploratory Studies in Hydraulics," *J. Hydr. Div. Proc. ASCE*, HY4, paper 1038, pp. 1~35.

Schrock, V. E., Revankar, S. T., Mannheimer, R. and Wang, C. H., 1986, "Small Break Critical Discharge - The Roles of Vapor and Liquid Entrainment in a Stratified Two-Phase Region Upstream of the Break," *NUREG/CR-4761*, U.S. Nuclear Regulatory Commission.

Smoglie, C., 1984, "Two-Phase Flow through Small Branches in a Horizontal Pipe with Stratified Flow," Kernforschungszentrum Karlsruhe, (KfK) 3861.

Yonomoto, T. and Tasaka, K., 1988, "New Theoretical Model for Two-Phase Flow Discharged from Stratified Two-Phase Region," *Nuclear Science and Technology*, Vol. 25, pp. 441~455.

Zuber, N., 1980, "Problems in Modeling of Small Break LOCA," *NUREG-0724*, U.S. Nuclear Regulatory Commission.